Three-dimensional static analysis of thick functionally graded plates using graded finite element method

Hassan Zafarmand and Mehran Kadkhodayan

Abstract

In this paper, a thick functionally graded plate based on three-dimensional equations of elasticity and subjected to nonuniform transverse loading is considered. The Young's modulus of the plate is assumed to be graded in the thickness direction according to a simple power law distribution in terms of the volume fractions of the constituents and the Poisson's ratio is assumed to be constant. Three-dimensional graded finite element method based on Rayleigh–Ritz energy formulation has been applied to study the static response of the plate. The plate deflection and in-plane stress for different values of the power law exponent, thickness-to-length ratio, and various boundary conditions have been investigated. To verify the presented method and data, the results are compared to published data.

Keywords

Functionally graded material, thick plate, three-dimensional theory of elasticity, three-dimensional graded finite element method

Date received: 13 April 2013; accepted: 11 September 2013

Introduction

In recent years, the composition of several different materials is often used in structural components in order to optimize the responses of structures subjected to thermal and mechanical loads. Functionally graded materials (FGMs) are suitable to achieve this purpose. They are composite materials, microscopically inhomogeneous, in which the mechanical properties vary smoothly and continuously from one surface to the other. This idea was used for the first time by Japanese researchers[1] which leads to the concept of FGMs. Most of the studies in this area are concerned with the thermoelastic and residual stress analysis.

The mechanical behavior of FGMs with various geometries and loading conditions has been studied by many researchers. Between the geometries that are studied, the plates are the most important because of great applications in engineering structures. It should be noted that the plate is a three-dimensional (3D) structure that one dimension is much smaller than the other dimensions. In 2D theories such as the Kirchhoff's classical plate theory or the shear deformations plate theories, to obtain a 2D formulation, various assumptions should be made. Clearly finding a solution for the plate in 2D formulation is easier. However, because of assumptions some errors occur in solutions, and these errors rise as the thickness of the plate increases. Unlike 2D solutions,

the 3D solution does not contain any simplification assumptions, so it is obvious that using 3D solutions would be more accurate than the solutions achieved by the 2D theories. Thus, in dealing with thick plates, for eliminating the lack of 2D theories, the 3D elasticity solution not only provides realistic and accurate results but also allows further physical insights, which cannot otherwise be estimated by plate theories.

Many papers studying static and dynamic response of functionally graded plates have been published recently. A critical literature review of these works is done by Jha et al.[2] Theoretical formulation, Navier's solutions of rectangular plates, and finite element models (FEMs) based on the third-order shear deformation plate theory (TSDT) are presented for the analysis of through-thickness functionally graded plates by Reddy.[3] Ferreira et al.[4] studied the static analysis of a simply supported functionally graded plate based on a TSDT by using a meshless method. Axisymmetric bending and stretching of functionally graded circular plates subjected to uniform transverse

Department of Mechanical Engineering, Ferdowsi University of Mashhad, Mashhad, Iran

Corresponding author:
Mehran Kadkhodayan, Department of Mechanical Engineering, Ferdowsi University of Mashhad, Mashhad 91775-1111, Iran.
Email: kadkhoda@um.ac.ir

loading based on fourth-order shear deformation plate theory have been investigated by Sahraee and Saidi.[5] Zenkour[6] presented the static response for a simply supported functionally graded rectangular plate subjected to a transverse uniform load based on the generalized shear deformation theory. Talha and Singh[7] studied free vibration and static analysis of functionally graded plates based on higher order shear deformation theory (HSDT) with a special modification in the transverse displacement in conjunction with FEMs. A focus on the bending analysis of functionally graded plates by an nth-order shear deformation theory and meshless global collocation method based on the thin plate spline radial basis function was made by Xiang and Kang[8] and the governing equations were derived by the principle of virtual work. Mantari et al.[9] presented an analytical solution to the static analysis of functionally graded plates using a recently developed HSDT[10] and provided detailed comparisons with other HSDTs available in the literature.[11–14] Moreover, in the case of thick functionally graded plates ($h/a \approx 0.2$), in which the 2D theories cannot lead to accurate results, several researches have been carried in the 3D approach. Pendhari et al.[15] presented a 3D mixed semianalytical and analytical solutions for a simply supported functionally graded rectangular plate. A 3D analysis by use of the radial basis function method is performed for orthotropic functionally graded rectangular plates with simply supported edges under static and dynamic loads by Wen et al.[16] Kashtalyan[17] suggested a 3D elasticity solution for a functionally graded simply supported plate under transversely distributed load. After that, Kashtalyan and Menshykova[18] extended this solution to a sandwich panel with functionally graded core. A differential quadrature and harmonic differential quadrature methods are used to obtain 3D elasticity solutions for bending and buckling of rectangular plate.[19] Vaghefi et al.[20] developed a version of meshless local Petrov–Galerkin (MLPG) method to obtain 3D static solutions for thick functionally graded plates. Rezaei Mojdehi et al.[21] presented the 3D static and dynamic analyses of thick functionally graded plates based on the MLPG. The Newmark time integration method is employed to obtain the answers in time domain.

The purpose of the current study is to investigate static response of a thick functionally graded plate. The Young's modulus of the plate is varied through the thickness with power law functions and the Poisson's ratio is assumed to be constant. The deflection and in-plane stress of the thick plate for different values of the power law exponent, thickness-to-length ratio, and various boundary conditions under nonuniform transverse loading are computed and compared. The difficulty in obtaining analytical solutions for response of graded material systems is due to the dispersive nature of the heterogeneous material systems.

Therefore, analytical or semianalytical solutions are available only through a number of problems with simple boundary conditions. Thus, in order to find the solution for a thick functionally graded plate subjected to any arbitrary loading function with various boundary conditions, powerful numerical methods such as graded finite element method (GFEM) are needed. The graded finite elements, which incorporate the material property gradient at the element level (material properties in each element are interpolated using linear shape functions), have been employed as a generalized isoparametric formulation. Some works can be found in the literature on modeling nonhomogenous structures by using GFEM.[22–24] In these researches, it is shown that the conventional FEM formulation causes a discontinuous stress field in the direction perpendicular to the material property gradation, while the graded elements give a continuous and smooth variation. Moreover, in the conventional FEM formulations, when material properties vary through the thickness, several elements need to be considered in the thickness in order to obtain converged results. But with the use of GFEM, the number of elements in the thickness reduces considerably. Thus, the run time and calculational efficiency in this approach (GFEM) do not differ significantly in comparison with the 2D approaches. Accordingly, the desired results are obtained without too much redundant computational costs.

Problem formulation

In this section the volume fraction distribution through the thickness of the plate is introduced. The 3D governing equations of equilibrium are obtained and graded finite element is utilized for modeling the nonhomogeneity of the material.

Material distribution and geometry of thick plate

Consider a thick functionally graded rectangular plate of uniform thickness h, length a, and width b as shown in Figure 1. The Cartesian coordinate system is shown such that the plane $z = 0$ and $z = h$ are the bottom and top surfaces of the plate, respectively. The plate is made up of a combined ceramic–metal material,
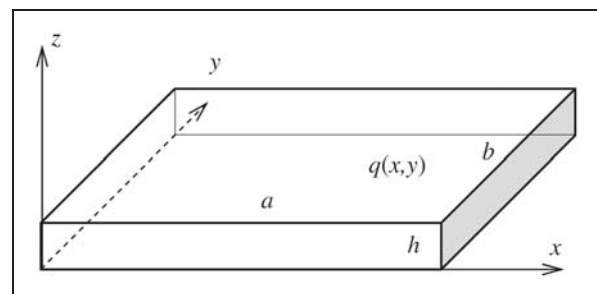
Figure 1. Thick rectangular plate.

the top surface of the plate is pure ceramic, and the bottom surface is pure metal. The material composition varying continuously along its thickness with a simple power law distribution is given as follows

$$\Re(z) = (\Re_c - \Re_m)\left(\frac{z}{h}\right)^n + \Re_m \qquad (1)$$

where $\Re$ is the material property and n is a nonnegative volume fraction exponent, subscripts "c" and "m" stand for ceramic and metal, respectively. It should be mentioned that the Poisson's ratio is assumed to be constant. This assumption is reasonable because of the small differences between the Poisson's ratios of basic materials.

Governing equations

The plate is subjected to the nonuniform loading on its top surface and the 3D equations of equilibrium in absence of body forces are

$$\frac{\partial \sigma_x}{\partial x} + \frac{\partial \tau_{xy}}{\partial y} + \frac{\partial \tau_{xz}}{\partial z} = 0 \qquad (2\text{-}1)$$

$$\frac{\partial \tau_{xy}}{\partial x} + \frac{\partial \sigma_y}{\partial y} + \frac{\partial \tau_{yz}}{\partial z} = 0 \qquad (2\text{-}2)$$

$$\frac{\partial \tau_{xz}}{\partial x} + \frac{\partial \tau_{yz}}{\partial y} + \frac{\partial \sigma_z}{\partial z} = 0 \qquad (2\text{-}3)$$

where σ_{ij} and τ_{ij} are components of normal and shear stresses, respectively.

The stress–strain relations from the Hook's law in matrix form are

$$\langle \sigma_{ij} \rangle = [D(z)]\langle \varepsilon_{ij} \rangle \qquad (3)$$

The stress and strain components and the coefficients of elasticity are

The strain–displacement equations based on theory of linear elasticity are

$$\begin{aligned}
\varepsilon_x &= \frac{\partial u}{\partial x}, & \gamma_{yz} &= \frac{\partial v}{\partial z} + \frac{\partial w}{\partial y} \\
\varepsilon_y &= \frac{\partial v}{\partial y}, & \gamma_{xz} &= \frac{\partial u}{\partial z} + \frac{\partial w}{\partial x} \\
\varepsilon_z &= \frac{\partial w}{\partial z}, & \gamma_{xy} &= \frac{\partial v}{\partial x} + \frac{\partial u}{\partial y}
\end{aligned} \qquad (7)$$

The boundary conditions used in this paper are defined as follows

$$CCCC: \begin{cases} x = 0, a \\ y = 0, b \end{cases} \rightarrow \big| u = 0, \quad v = 0, \quad w = 0$$
$$(8\text{-}1)$$

$$SSSS: \begin{cases} x = 0, a \rightarrow \big| v = 0, \quad w = 0 \\ y = 0, b \rightarrow \big| u = 0, \quad w = 0 \end{cases} \qquad (8\text{-}2)$$

$$CSCS: \begin{cases} x = 0, a \rightarrow \big| u = 0, \quad v = 0, \quad w = 0 \\ y = 0, b \rightarrow \big| u = 0, \quad w = 0 \end{cases}$$
$$(8\text{-}3)$$

$$CFCF1: \big\{ y = 0, b \rightarrow \big| u = 0, \quad v = 0, \quad w = 0$$
$$(8\text{-}4)$$

$$CFCF2: \big\{ x = 0, a \rightarrow \big| u = 0, \quad v = 0, \quad w = 0$$
$$(8\text{-}5)$$

where u, v, and w are displacement components.

Graded finite element modeling

In order to solve the governing equations, the isoparametric finite element method with graded element properties is used. For this purpose the variational formulation is considered. In conventional finite elem-

$$\langle \sigma_{ij} \rangle = \langle \sigma_x, \sigma_y, \sigma_z, \tau_{yz}, \tau_{xz}, \tau_{xy} \rangle^T \qquad (4)$$

$$\langle \varepsilon_{ij} \rangle = \langle \varepsilon_x, \varepsilon_y, \varepsilon_z, \gamma_{yz}, \gamma_{xz}, \gamma_{xy} \rangle^T \qquad (5)$$

$$[D] = \frac{E(z)}{(1+v)(1-2v)} \begin{bmatrix} 1-v & v & v & 0 & 0 & 0 \\ v & 1-v & v & 0 & 0 & 0 \\ v & v & 1-v & 0 & 0 & 0 \\ 0 & 0 & 0 & (1-2v)/2 & 0 & 0 \\ 0 & 0 & 0 & 0 & (1-2v)/2 & 0 \\ 0 & 0 & 0 & 0 & 0 & (1-2v)/2 \end{bmatrix} \qquad (6)$$

where v denotes the Poisson's ratio and assumed to be constant and E is Young's modulus that depends on z coordinate.

ent formulations, a predetermined set of material properties is used for each element such that the property field is constant within an individual element.

For modeling a continuously nonhomogeneous material, the material property function must be discretized according to the size of elements mesh. This approximation can provide significant discontinuities. Based on these facts the graded finite element is strongly preferable for modeling of the present problem.

Hamilton's principle for the present problem is

$$\int_{t_1}^{t_2} \delta(U - W)\mathrm{d}t = 0 \tag{9}$$

where U and W are potential energy and virtual work done by surface tractions, respectively. These functions and their variations are

$$U = \int_V \sigma_{ij}\varepsilon_{ij}\,\mathrm{d}V \tag{10-1}$$

$$\delta U = \int_V \sigma_{ij}\delta\varepsilon_{ij}\,\mathrm{d}V \tag{10-2}$$

$$W = \int_A p_i u_i\,\mathrm{d}A \tag{11-1}$$

$$\delta W = \int_A p_i \delta u_i\,\mathrm{d}A \tag{11-2}$$

where V and A are the volume and area of the domain under consideration and p_i is the component of surface tractions.

Substituting equations (10) and (11) in equation (9), applying side conditions $\delta u_i(t_1) = \delta u_i(t_2) = 0$, and using part integration give

$$\int_V \sigma_{ij}\delta\varepsilon_{ij}\,\mathrm{d}V = \int_A p_i \delta u_i\,\mathrm{d}A \tag{12}$$

The strain–displacement equations based on theory of linear elasticity in the matrix form can be written as

$$\{\varepsilon\} = [d]\{f\} \tag{13}$$

where

$$[d] = \begin{bmatrix} \partial/\partial x & 0 & 0 \\ 0 & \partial/\partial y & 0 \\ 0 & 0 & \partial/\partial z \\ 0 & \partial/\partial z & \partial/\partial y \\ \partial/\partial z & 0 & \partial/\partial x \\ \partial/\partial y & \partial/\partial x & 0 \end{bmatrix} \tag{14}$$

and

$$\{f\} = \begin{Bmatrix} u \\ v \\ w \end{Bmatrix} \tag{15}$$
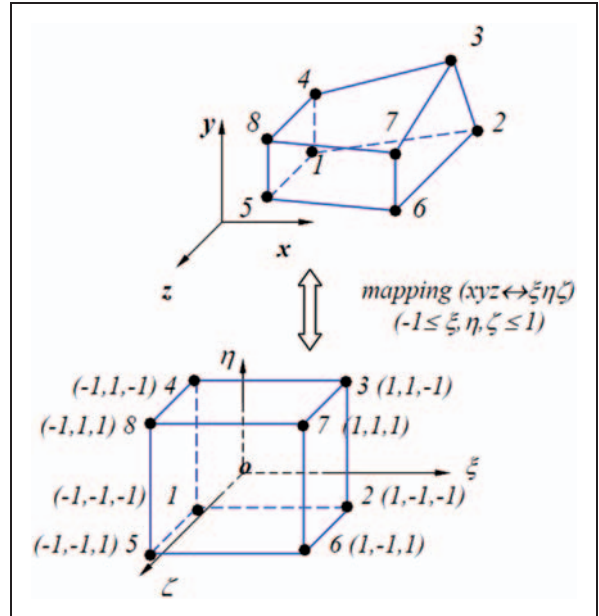
Figure 2. Mapping to local coordinate.

The plate is divided into a number of linear hexahedron or break elements, each of them has eight nodes. For convenience the local coordinate is used and its variables (ξ, η, ζ) are between -1 to $+1$ as shown in Figure 2. For element (e), the displacements in three directions are approximated as follows

$$\{f\}^{(e)} = [N]^{(e)}\{Q\}^{(e)} \tag{16}$$

where $[N]$ is the matrix of linear shape function in local coordinate and $\{Q\}^{(e)}$ is the nodal displacement vector of the element that are as

$$\{Q\}^{(e)} = \langle U_1, V_1, W_1, U_2, V_2, W_2, \ldots, U_8, V_8, W_8 \rangle^T \tag{17}$$

$$[N]^{(e)}$$
$$= \begin{bmatrix} N_1 & 0 & 0 & N_2 & 0 & 0 & \ldots & N_8 & 0 & 0 \\ 0 & N_1 & 0 & 0 & N_2 & 0 & \ldots & 0 & N_8 & 0 \\ 0 & 0 & N_1 & 0 & 0 & N_2 & \ldots & 0 & 0 & N_8 \end{bmatrix}_{3*24} \tag{18}$$

Substituting equation (16) in equation (13) gives the strain matrix of element (e) as

$$\{\varepsilon\}^{(e)} = [d][N]^{(e)}\{Q\}^{(e)} \tag{19}$$

$$[B]^{(e)} = [d][N]^{(e)} \tag{20}$$

$$\{\varepsilon\}^{(e)} = [B]^{(e)}\{Q\}^{(e)} \tag{21}$$

The components of matrix N and B are given in Appendix 2.

Applying Hamilton's principle for each element and using equations (3) and (21), it can be achieved that

$$
\begin{aligned}
&\delta\{Q^{(e)}\}^T\left[\int_{V^{(e)}}[B]^T[D][B]\mathrm{d}V\right]\{Q^{(e)}\} \\
&= \delta\{Q^{(e)}\}^T\left[\int_{S^{(e)}}[N]^T\{P\}\mathrm{d}S\right]
\end{aligned} \tag{22}
$$

where $V^{(e)}$, $S^{(e)}$, and $\{P\}$ are volume of element, area under pressure, and vector of surface tractions, respectively.

To treat the material inhomogeneity by using the GFEM, in each element we have

$$
\Im = \sum_{i=1}^{8}\Im_i N_i \tag{23}
$$

Thus in each element, the elastic modulus is a function of local coordinate as

$$
E^{(e)} = E(\xi, \eta, \zeta) \tag{24}
$$

Substituting equation (24) into equation (22) gives

$$
[K]^{(e)}\{Q\} = \{F\}^{(e)} \tag{25}
$$

where

$$
[K]^{(e)} = \int_V [B]^T[D][B]\mathrm{d}V \tag{26}
$$

$$
\{F\}^{(e)} = \int_{S^{(e)}}[N]^T\{P\}\mathrm{d}S \tag{27}
$$

To find the stiffness matrix, the integral must be taken over the elements' volume which is evaluated by numerical integration for each element. First the integral is taken to the local coordinate as below

$$
\begin{aligned}
I &= \int_{V^{(e)}} f(X)\mathrm{d}V \\
&= \iiint_{V^{(e)}} f[X(\xi, \eta, \zeta)]\det[J(\xi, \eta, \zeta)]\,\mathrm{d}\xi\,\mathrm{d}\eta\,\mathrm{d}\zeta \\
&= \iiint_{V^{(e)}} g(\xi, \eta, \zeta)\,\mathrm{d}\xi\,\mathrm{d}\eta\,\mathrm{d}\zeta
\end{aligned} \tag{28}
$$

where J is Jacobian matrix and is introduced in Appendix 2. In this way, the integration domain is identical for all elements belonging to the same type. Now, the analytical integration is approximated by a numerical integration scheme. This basically means that the integral in equation (28) is replaced by a linear combination of function values at specific locations, the so-called integration points, within the domain of integration

$$
\iiint_{V^{(e)}} g(\xi, \eta, \zeta)\mathrm{d}\xi\,\mathrm{d}\eta\,\mathrm{d}\zeta \approx \sum_{i=1}^{N} g(\xi_i, \eta_i, \zeta_i)\psi_i \tag{29}
$$

The value of the weights, the location of the integration points, and their number constitute together an integration scheme. Different schemes lead to different calculational expenditure and different accuracy. For finite element calculations, the Gauss schemes are very popular, because of their high accuracy compared to the numerical expenditure.[25]

In this case the $2 \times 2 \times 2$ scheme which represents full integration for a linear element (eight-node brick) is used. The location of integration point and their weights are defined as

$$
\begin{aligned}
\psi_i &= 1 \\
\xi_i, \eta_i, \zeta_i &= \left(\pm\frac{1}{\sqrt{3}}, \pm\frac{1}{\sqrt{3}}, \pm\frac{1}{\sqrt{3}}\right)
\end{aligned} \tag{30}
$$

Now by assembling the element matrices, the global equilibrium equations for the functionally graded plate can be obtained as

$$
[K]\{Q\} = \{F\} \tag{31}
$$

Once the finite element equations are established, the displacements and stresses would be found by equations (31) and (3), respectively.

Results and discussions

Validation

To validate the current work, the data of a functionally graded plate can be used.[6] The plate is square ($a = b$) with a thickness-to-length ratio of 0.1 ($h/a = 0.1$) and consists of aluminum and alumina as its components. The modulus of elasticity at the top surface (alumina) is $E_c = 380\,\text{GPa}$, at the bottom surface (aluminum) is $E_m = 70\,\text{GPa}$, and Poisson's ratio is selected constant for both and equal to 0.3. Material distribution is assumed to be varied in thickness from metal (aluminum) at the bottom surface to ceramic (alumina) at the top surface with a power law function. The boundary conditions are simply supported and the load is sinusoidal as below

$$
q(x, y) = -q_0 \sin\left(\frac{\pi x}{a}\right)\sin\left(\frac{\pi y}{b}\right), \quad q_0 = 10^6\,\text{Pa} \tag{32}
$$

The comparison of the nondimensional parameters defined in Ref. 6 with the results of the present study is given in Table 1 and a good agreement between these two results is observed.

$$\bar{w} = \frac{10h^3 E_c}{a^4 q_0} w\left(\frac{a}{2}, \frac{b}{2}\right) \tag{33-1}$$

$$\bar{\sigma}_x = \frac{h}{aq_0} \sigma_x\left(\frac{a}{2}, \frac{b}{2}, h\right) \tag{33-2}$$

Numerical results and discussions

A thick functionally graded square plate of side equal to 1 m ($a = b = 1$ m) is considered here. The nonuniform load is taken as

$$q(x, y) = -q_0 x^2 \sin(\pi y) \tag{34}$$

Table 1. Nondimensional deflection and stress compared to Ref. 6.

	$\bar{w}$		$\bar{\sigma}_x$	
n	Ref. 6	Present	Ref. 6	Present
Ceramic	0.2960	0.2921	1.9955	2.02
2	0.7573	0.7490	3.6094	3.6682
4	0.8819	0.8855	4.0693	4.008
Metal	1.6070	1.6021	1.9955	2.02

where

$$q_0 = 10^6 \, \text{Pa} \tag{35}$$

The distribution schematic of nonuniform load is shown in Figure 3.

First, the influence of power law exponent (n) and thickness-to-length ratio (h/a) on maximum deflection and distribution of σ_x in the thickness direction of the plate is studied. The boundary condition is assumed to be *CCCC*. Figure 4 shows the influence of power law exponent on maximum deflection of the plate with a constant thickness-to-length ratio of 0.1. As it can be seen, the maximum deflection increases when power law exponent rises, as a result of the fact that when n raises the material properties approach metal, thus the elasticity modulus decreases.

The effect of thickness-to-length ratio of the plate on maximum deflection with $n = 2$ is shown in Figure 5. The figure shows, while the thickness-to-length ratio increases, the maximum deflection decreases due to growth of stiffness of the plate.

Figures 6 and 7 illustrate the effect of power law exponent and thickness-to-length ratio (h/a) on the variation of σ_x through the thickness of the plate. According to these figures, there is compression at the top surface and tension at the bottom surface. Moreover, the neutral plane (where σ_x vanishes) goes upper with the increase of power law exponent and remains unchanged when thickness-to-length ratio varies.

Now the effect of various boundary conditions for a thick functionally graded plate with a constant power law exponent and thickness-to-length ratio is investigated. The load distribution is as shown in Figure 3.
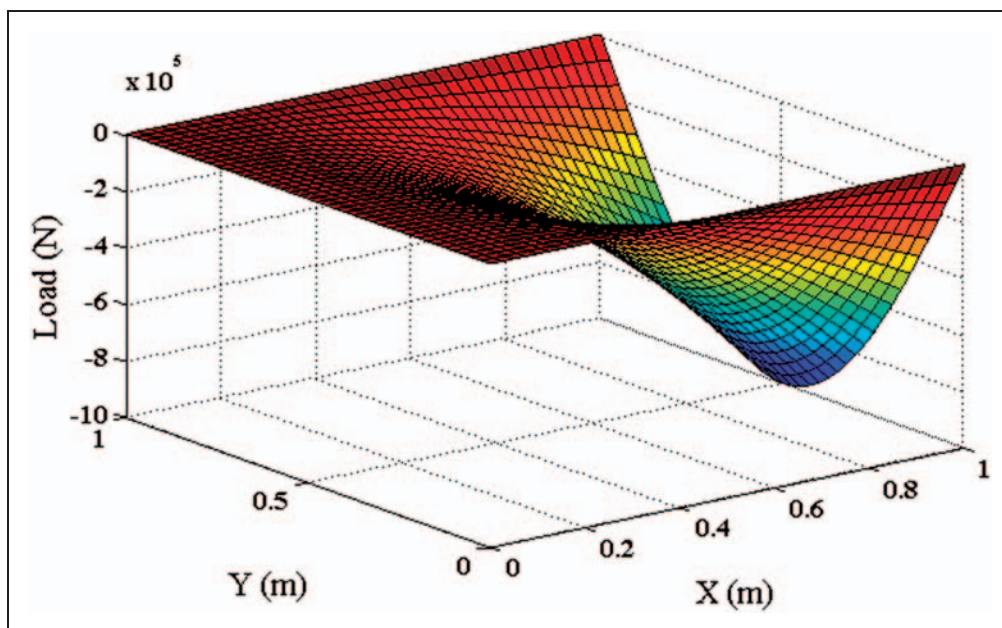
Figure 3. Nonuniform load.
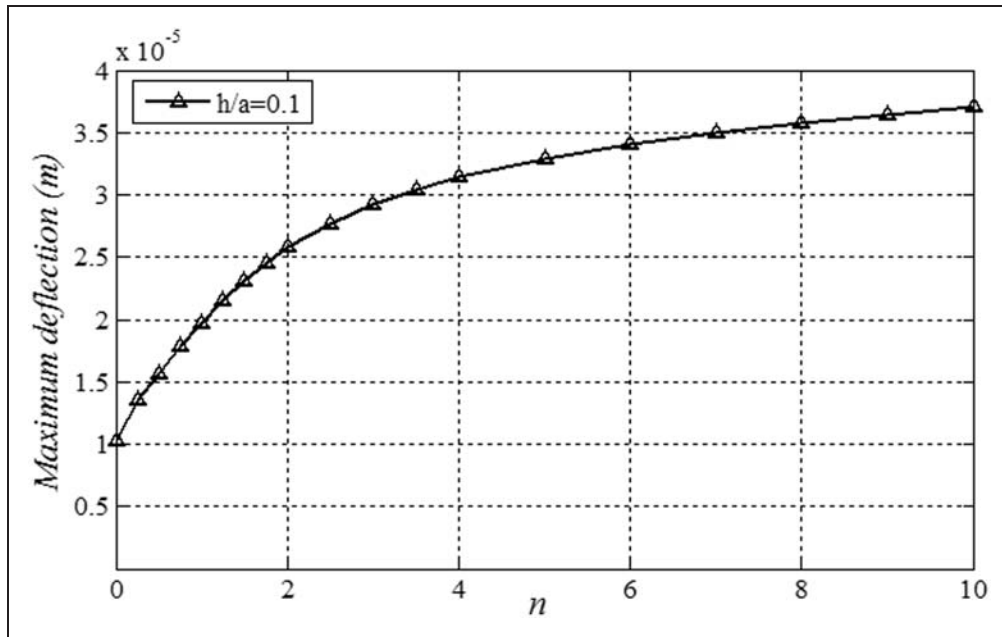
Figure 4. Influence of power law exponent on maximum deflection ($h/a = 0.1$).
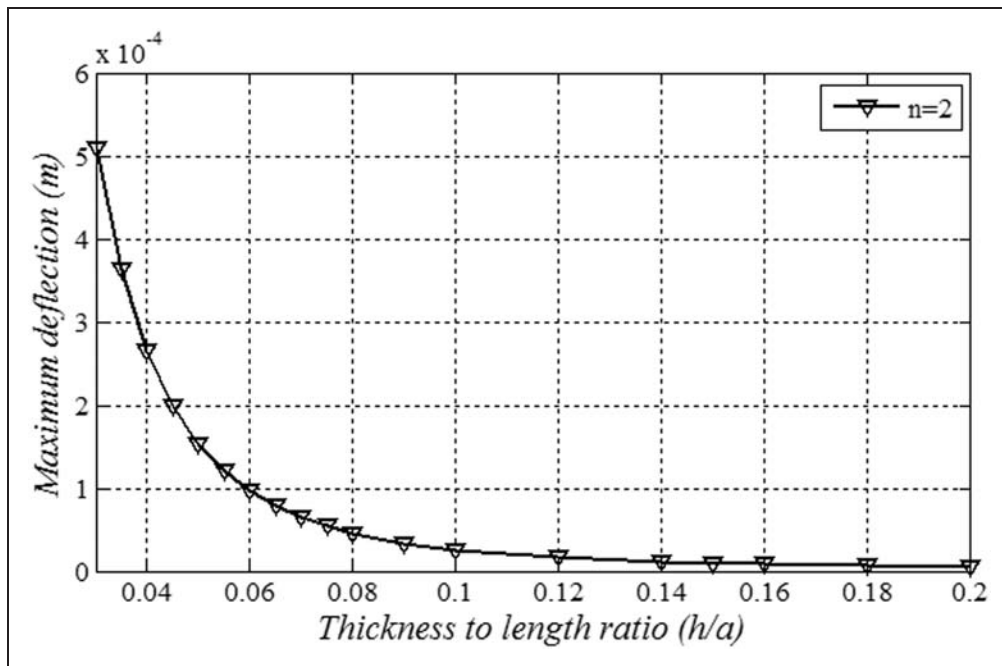
Figure 5. Influence of thickness-to-length ratio on maximum deflection ($n = 2$).

The power law exponent (n) and thickness-to-length ratio (h/a) are assumed to be 2 and 0.1, respectively. The deflection distributions in the middle plane of the plate with mentioned boundary conditions in equation (8) are shown in Figure 8(a) to (e).

It is seen that with the increase of plate's degrees of freedom, the maximum deflection rises, as presented in Table 2. The deflection distribution in the boundary condition *CFCF1* and *CFCF2* differs as a result of nonuniform loading.

Figure 9 shows the effect of boundary conditions on variation of σ_x with a constant n and h/a. It is obvious that the neutral plane is independent of boundary conditions.
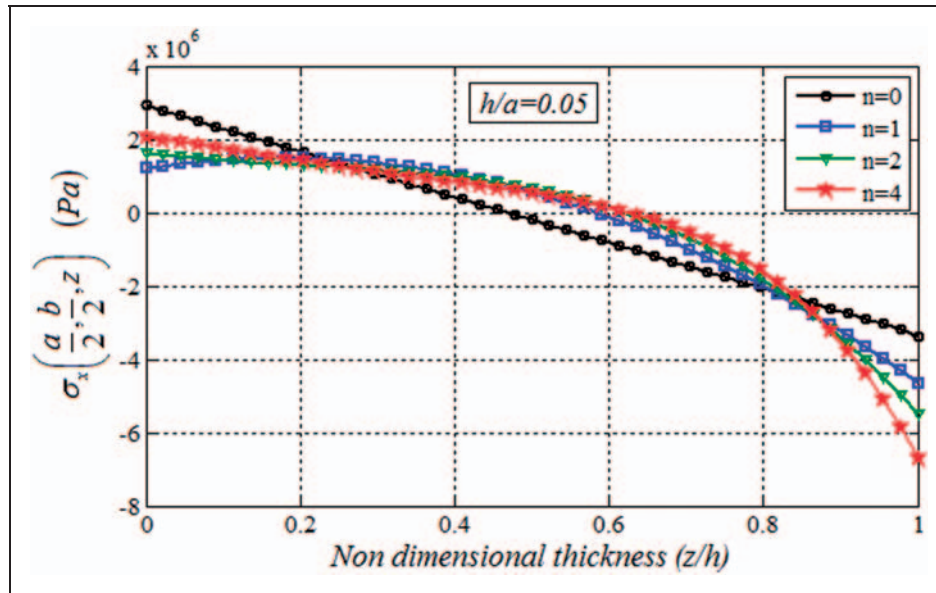
Figure 6. Effect of power law exponent on variation of σ_x ($h/a = 0.05$).
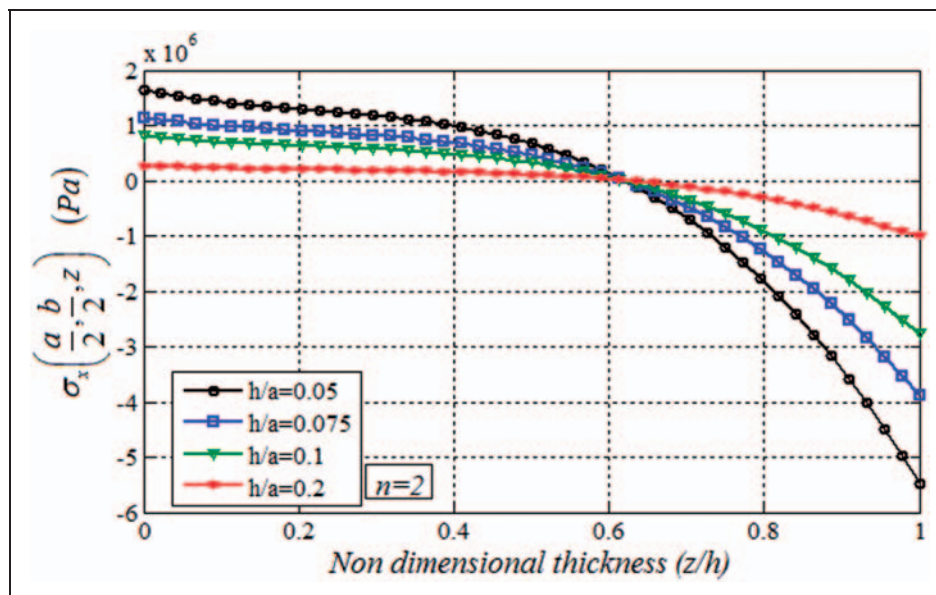
Figure 7. Effect of thickness-to-length ratio (h/a) on variation of σ_x ($n = 2$).

Conclusions

The main purpose of the present paper was to study the static analysis of thick functionally graded plate. The 3D GFEM and Rayleigh–Ritz energy formulation was applied. The proposed method was validated by the result of a functionally graded plate under sinusoidal loading which was extracted from published literature. The comparisons between the results show that the present method has a good agreement with the existing results. The effects of thickness-to-length ratio of the plate and the power law exponent on the deflection and

stress were presented for a thick functionally graded plate. Additionally, the influences of different boundary conditions on the deflection and in-plane stress of the plate were studied. The obtained results denote that the maximum stress, stress distribution, and maximum deflection can be controlled by the material distribution. Advantages of the present method are its applicability to any FGM model, applying any boundary condition and loading, and supporting any 3D geometry. Moreover, the results demonstrate that using linear shape functions to interpolate material properties in each element provide smoother and more accurate results than homogeneous elements.
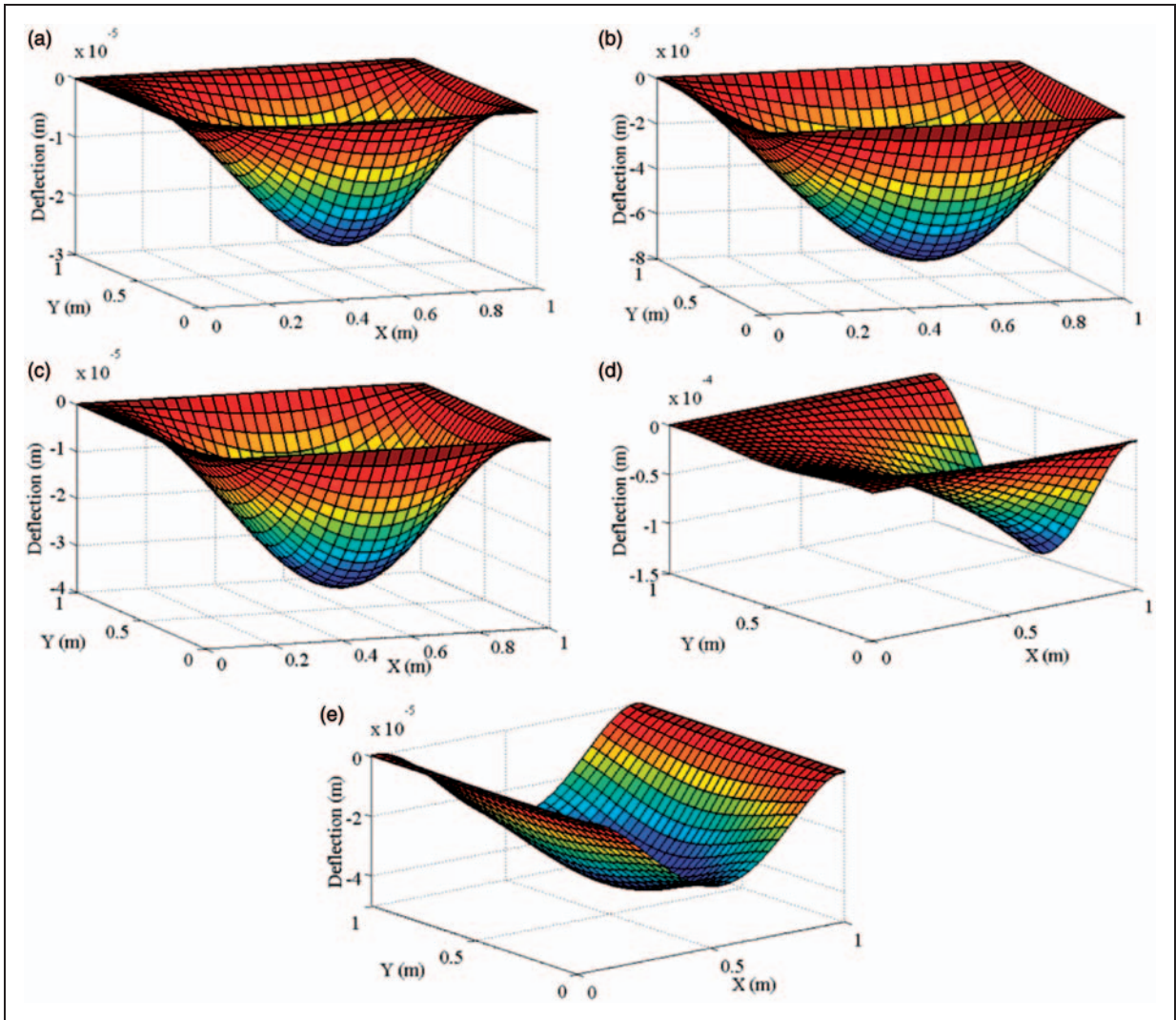
Figure 8. The deflection distributions for various boundary conditions: (a) *CCCC*, (b) *SSSS*, (c) *CSCS*, (d) *CFCF1* and (e) *CFCF2*.

Table 2. Maximum deflection in various boundary conditions.

B.C	CCCC	CSCS	CFCF2	SSSS	CFCF1
w_{max} (m)	2.58e-5	3.54e-5	4.12e-5	7.22e-5	1.47e-4
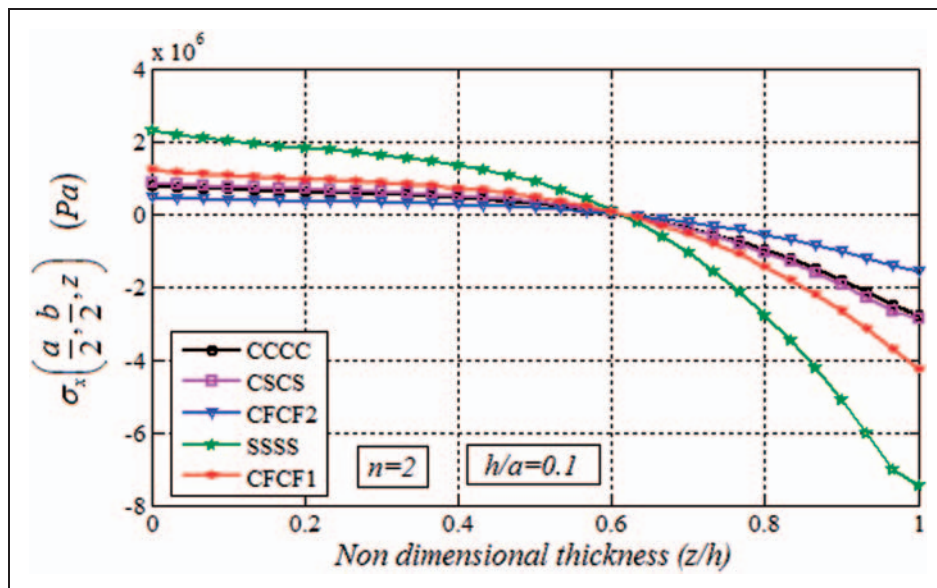
Figure 9. Effect of boundary conditions on variation of σ_x ($n = 2$, $h/a = 0.1$).

References

1. Koizumi M. The concept of FGM. *Ceram Trans Funct Grad Mater* 1993; 34: 3–10.
2. Jha DK, Kant T and Singh RK. A critical review of recent research on functionally graded plates. *Compos Struct* 2012; 96: 833–849.
3. Reddy JN. Analysis of functionally graded plates. *Int J Numer Meth Eng* 2000; 47: 663–684.
4. Ferreira AJM, Batra RC, Roque CMC, et al. Static analysis of functionally graded plates using third-order shear deformation theory and a meshless method. *Compos Struct* 2005; 69: 449–457.
5. Sahraee S and Saidi AR. Axisymmetric bending analysis of thick functionally graded circular plates using fourth-order shear deformation theory. *Eur J Mech A/Solids* 2009; 28: 974–984.
6. Zenkour AM. Generalized shear deformation theory for bending analysis of functionally graded plates. *Appl Math Model* 2006; 30: 67–84.
7. Talha M and Singh BN. Static response and free vibration analysis of FGM plates using higher order shear deformation theory. *Appl Math Model* 2010; 34: 3991–4011.
8. Xiang S and Kang G. A nth-order shear deformation theory for the bending analysis on the functionally graded plates. *Eur J Mech A/Solids* 2013; 37: 336–343.
9. Mantari JL, Oktem AS and Soares CG. Bending response of functionally graded plates by using a new higher order shear deformation theory. *Compos Struct* 2012; 94: 714–723.
10. Mantari JL, Oktem AS and Soares CG. A new higher order shear deformation theory for sandwich and composite laminated plates. *Compos Part B* 2012; 43: 1489–1499.
11. Karama M, Afaq KS and Mistou S. A new theory for laminated composite plates. *Proc IMechE, Part L: J Materials: Design and Applications* 2009; 223: 53–62.
12. Reddy JN and Liu CF. A higher order shear deformation theory of laminated elastic shells. *Int J Eng Sci* 1985; 23: 319–330.
13. Soldatos KP. A transverse shear deformation theory for homogeneous monoclinic plates. *Acta Mech* 1992; 94: 195–220.
14. Touratier M. An efficient standard plate theory. *Int J Eng Sci* 1991; 29: 901–916.
15. Pendhari SS, Kant T, Desai YM, et al. Static solution for functionally graded simply supported plates. *Int J Mech Mater Des* 2012; 8: 51–69.
16. Wen PH, Sladek J and Sladek V. Three dimensional analysis of functionally graded plates. *Int J Numer Meth Eng* 2011; 87: 923–942.
17. Kashtalyan M. Three-dimensional elasticity solution for bending of functionally graded plates. *Eur J Mech A/Solids* 2004; 23: 853–864.
18. Kashtalyan M and Menshykova M. Three dimensional elasticity solution for sandwich panels with a functionally graded core. *Compos Struct* 2008; 87: 36–43.
19. Liew KM, Teo TM and Han JB. Three dimensional static solutions of rectangular plates by variant differential quadrature method. *Int J Mech Sci* 2001; 43: 1611–1628.
20. Vaghefi R, Baradaran GH and Koohkan H. Three-dimensional static analysis of thick functionally graded plates by using meshless local Petrov–Galerkin (MLPG) method. *Eng Anal Bound Elem* 2010; 34: 564–573.
21. Rezaei Mojdehi A, Darvizeh B, Basti A, et al. Three dimensional static and dynamic analysis of thick functionally graded plates by the meshless local Petrov–Galerkin (MLPG) method. *Eng Anal Bound Elem* 2011; 35: 1168–1180.
22. Kim JH and Paulino GH. Isoparametric graded finite elements for nonhomogeneous isotropic and ortho-tropic materials. *J Appl Mech* 2002; 69: 502–514.
23. Zhang Z and Paulino GH. Wave propagation and dynamic analysis of smoothly graded heterogeneous continua using graded finite elements. *Int J Solids Struct* 2007; 44: 3601–3626.
24. Ashrafi H, Asemi K, Shariyat M, et al. Two-dimensional modelling of heterogeneous structures using graded finite element and boundary element methods. *Meccanica* 2012; 48: 663–680.
25. Dhondt G. *The finite element method for three-dimensional thermo mechanical applications*. UK: John Wiley & Sons Ltd, 2004.
26. Zienkiewicz OC and Taylor RL. *The finite element method for solid and structural mechanics*. 6th ed. Oxford: Elsevier Butterworth-Heinemann, 2005.
27. Eslami MR. *A first course in finite element analysis*. 1st ed. Tehran: Amirkabir University of Technology Press, 2003.

Appendix 1

Notation

a	length of the plate
b	width of the plane
E	elasticity modulus
$\boldsymbol{F}$	force vector
h	thickness of the plate
$\boldsymbol{J}$	Jacobian matrix
$\boldsymbol{K}$	stiffness matrix
n	power law exponent
N_i	shape functions
$\boldsymbol{P}$	surface traction vector
q	nonuniform load
$\boldsymbol{Q}$	nodal displacement vector
u	displacement in x direction
U	potential energy
v	displacement in y direction
w	displacement in z direction
W	virtual work
$\Re$	material properties in plate
$\Im$	material properties in element
γ_{ij}	shear strains
ε_{ij}	normal strains
ζ	local coordinate

η local coordinate
ν Poisson's ratio
ξ local coordinate
σ_{ij} normal stresses
τ_{ij} shear stresses

Appendix 2

The linear shape functions are[26]

$$N_1 = (1 - \xi)(1 - \eta)(1 - \zeta)/8 \tag{36}$$

$$N_2 = (1 + \xi)(1 - \eta)(1 - \zeta)/8 \tag{37}$$

$$N_3 = (1 + \xi)(1 + \eta)(1 - \zeta)/8 \tag{38}$$

$$N_4 = (1 - \xi)(1 + \eta)(1 - \zeta)/8 \tag{39}$$

$$N_5 = (1 - \xi)(1 - \eta)(1 + \zeta)/8 \tag{40}$$

$$N_6 = (1 + \xi)(1 - \eta)(1 + \zeta)/8 \tag{41}$$

$$N_7 = (1 + \xi)(1 + \eta)(1 + \zeta)/8 \tag{42}$$

$$N_8 = (1 - \xi)(1 + \eta)(1 + \zeta)/8 \tag{43}$$

and components of matrix $[B]$ are

$$[B]^{(e)} = \begin{bmatrix} \partial N_1/\partial x & 0 & 0 & \ldots & \partial N_8/\partial x & 0 & 0 \\ 0 & \partial N_1/\partial y & 0 & \ldots & 0 & \partial N_8/\partial y & 0 \\ 0 & 0 & \partial N_1/\partial z & \ldots & 0 & 0 & \partial N_8/\partial z \\ 0 & \partial N_1/\partial z & \partial N_1/\partial y & \ldots & 0 & \partial N_8/\partial z & \partial N_8/\partial y \\ \partial N_1/\partial z & 0 & \partial N_1/\partial x & \ldots & \partial N_8/\partial z & 0 & \partial N_8/\partial x \\ \partial N_1/\partial y & \partial N_1/\partial x & 0 & \ldots & \partial N_8/\partial y & \partial N_8/\partial x & 0 \end{bmatrix}_{6*24} \tag{44}$$

Because the shape functions are functions of local variables (ξ, η, ζ), to differentiate them with respect to Cartesian variables (x, y, z), we should use the chain rule as below[27]

$$\begin{bmatrix} \partial N_i/\partial \xi \\ \partial N_i/\partial \eta \\ \partial N_i/\partial \zeta \end{bmatrix} = \begin{bmatrix} \partial x/\partial \xi & \partial y/\partial \xi & \partial z/\partial \xi \\ \partial x/\partial \eta & \partial y/\partial \eta & \partial z/\partial \eta \\ \partial x/\partial \zeta & \partial y/\partial \zeta & \partial z/\partial \zeta \end{bmatrix} \begin{bmatrix} \partial N_i/\partial x \\ \partial N_i/\partial y \\ \partial N_i/\partial z \end{bmatrix}$$

$$= J \begin{bmatrix} \partial N_i/\partial x \\ \partial N_i/\partial y \\ \partial N_i/\partial z \end{bmatrix} \tag{45}$$

$$\begin{bmatrix} \partial N_i/\partial x \\ \partial N_i/\partial y \\ \partial N_i/\partial z \end{bmatrix} = J^{-1} \begin{bmatrix} \partial N_i/\partial \xi \\ \partial N_i/\partial \eta \\ \partial N_i/\partial \zeta \end{bmatrix} \tag{46}$$

where J is the Jacobian matrix. By use of the shape functions, we could write the Cartesian variables (x, y, z) as function of local variables (ξ, η, ζ)

$$x = \sum_{i=1}^{8} N_i x_i \tag{47}$$

$$y = \sum_{i=1}^{8} N_i y_i \tag{48}$$

$$z = \sum_{i=1}^{8} N_i z_i \tag{49}$$

where (x_i, y_i, z_i) and N_i are locations of element nodes and shape functions, respectively. Hence, the Jacobian matrix and $[B]$ would be obtained.